JOURNAL OF NEUROTRAUMA 34:2342–2352 (August 1, 2017)

DOI: 10.1089/neu.2016.4915

Compression Decreases Anatomical and Functional Recovery and Alters Inflammation after Contusive Spinal Cord Injury

Michael B. Orr,[1,3,*] Jennifer Simkin,[1,2,*] William M. Bailey,[1] Neha S. Kadambi,[4] Anna Leigh McVicar,[1] Amy K. Veldhorst,[1] and John C. Gensel[1]

Abstract

Experimental models of spinal cord injury (SCI) typically utilize contusion or compression injuries. Clinically, however, SCI is heterogeneous and the primary injury mode may affect secondary injury progression and neuroprotective therapeutic efficacy. Specifically, immunomodulatory agents are of therapeutic interest because the activation state of SCI macrophages may facilitate pathology but also improve repair. It is unknown currently how the primary injury biomechanics affect macrophage activation. Therefore, to determine the effects of compression subsequent to spinal contusion, we examined recovery, secondary injury, and macrophage activation in C57/BL6 mice after SCI with or without a 20 sec compression at two contusion impact forces (50 and 75 kdyn). We observed that regardless of the initial impact force, compression increased tissue damage and worsened functional recovery. Interestingly, compression-dependent damage is not evident until one week after SCI. Further, compression limits functional recovery to the first two weeks post-SCI; in the absence of compression, mice receiving contusion SCI recover for four weeks. To determine whether the recovery plateau is indicative of compression-specific inflammatory responses, we examined macrophage activation with immunohistochemical markers of purportedly pathological (CD86 and macrophage receptor with collagenous structure [MARCO]) and reparative macrophages (arginase [Arg1] and CD206). We detected significant increases in macrophages expression of MARCO and decreases in macrophage Arg1 expression with compression, suggesting a biomechanical-dependent shift in SCI macrophage activation. Collectively, compression-induced alterations in tissue and functional recovery and inflammation highlight the need to consider the primary SCI biomechanics in the design and clinical implementation of immunomodulatory therapies.

Keywords: infinite horizons; inflammation; mice; microglia

Introduction

Spinal cord injury (SCI) is heterogeneous in nature and triggers a broad spectrum of secondary physiological responses that are beneficial or detrimental to recovery. In animal models, a number of therapeutic interventions are effective at altering the secondary injury progression and increasing recovery; however, translation of these therapies into clinical application is challenging. An obstacle to developing treatments is the heterogeneity of the primary injury, which involves a diversity of biomechanical factors including varying degrees of contusion and compression. Efforts to maximize control of experimental systems often isolate biomechanical variables (e.g., testing only compression or contusion), but these models potentially miss subtle variations in secondary injury progression because of the primary mode of injury.[1] Understanding the effects of injury biomechanics on secondary injury progression is necessary for effective implementation and translation from animal models to clinical therapies.

The SCI field has extensively described locomotor dysfunction and tissue damage resulting from varying magnitudes of isolated contusion or compression injury.[2–6] Considering translation of the models, though, clinical cases commonly exhibit combinations of biomechanical variables. The effects of varying degrees of compression in contusion SCI have been investigated,[7–12] but the effect of compression at variable contusion forces is not well understood. Specifically, it is difficult to separate the inherent effects of compression independently from the increased injury severity caused by the combined contusion and compression SCI. We have used the

[1]Spinal Cord and Brain Injury Research Center and the Department of Physiology, [2]Department of Biology, [3]Integrated Biomedical Sciences Graduate Program, the University of Kentucky, Lexington, Kentucky.
[4]Math, Science, and Technology Center Program, Dunbar High School, Lexington, Kentucky.
*These authors contributed equally to this article.

Infinite Horizons (IH) SCI impactor[2] to alter compression after a controlled spinal contusion to characterize the functional and anatomical outcomes from compression across different contusion severities. This approach provides the basis for studying the influence of these varying SCI biomechanics on secondary injury cascades.

One key aspect of secondary injury cascades is the inflammatory response to SCI. Many factors contribute to the recruitment and activation of immune cells such as microglia and monocyte-derived macrophages. Once activated and recruited to the damaged spinal cord, microglia and macrophages have substantial overlap in morphology, receptors, and cytokines (thus, both will be referred to hereafter simply as macrophages). These macrophages can adopt cytotoxic and neuroprotective phenotypes with profound impacts on overall outcomes from SCI.[13–15] A number of therapies are being developed to drive macrophages toward reparative phenotypes[16]; however, little is known about how the initial biomechanics of SCI alters intraspinal macrophage activation.

The aim of this study was to examine how the addition of compression to a contusion injury, regardless of impact force, alters functional and anatomical recovery and intraspinal inflammation. Here we find that compression in moderate (50 kdyn force) and severe (75 kdyn force) contusion injuries decreases both tissue sparing and functional recovery, and we report a compression-induced blunting of functional recovery regardless of contusion severity. We also provide the first evidence that these biomechanics of SCI contribute to macrophage polarization/activation states. Specifically, compression, independent of contusion force, polarized macrophages toward proinflammatory activation as indicated by increased macrophage receptor with collagenous structure (MARCO) expression and decreased arginase 1 (Arg1) expression within the injured spinal cord. The inflammatory shift coincided with a compression-specific plateau in functional recovery. This study provides insight into the effects of SCI biomechanics on secondary injury and highlights the need to consider the primary injury biomechanics in the design and clinical implementation of immunomodulatory therapies for SCI.

Methods

Experimental design

Mouse spinal cord injuries were produced by delivering 50 kdyn or 75 kdyn force contusions to the T9 thoracic spinal cord with or without 20 sec of sustained compression. Four different injury groups were generated: (1) 75 dyn (contusion), (2) 75 kdyn +20 sec (of spinal cord compression), (3) 50 kdyn, and (4) 50 kdyn +20 sec. At 3, 7, and 14 days post-injury (dpi), $n = 4$–6 animals/group were sacrificed, and tissue was harvested for histological evaluation. Locomotor analysis using the Basso Mouse Scale (BMS) was conducted on a separate set of animals (n = 10/group) over the course of four weeks. At 28 dpi, these animals were sacrificed and spinal cord sections generated for histological analyses. Staining and analyses were performed to track inflammatory response at 7 and 14 dpi and anatomical recovery at 3, 7, 14, and 28 dpi.

Animals

Experiments were performed using 90 3–4 month old female C57BL/6 mice (Jackson Laboratory, Bar Harbor, Maine). Animals were housed in individually ventilated cages with *ad libitum* access to food and water. All procedures were performed in accordance with the guidelines of the Office of Responsible Research Practices and with the approval of the Institutional Animal Care and Use Committee at the University of Kentucky.

SCI

Mice were anesthetized via intraperitoneal (ip) injections of ketamine (100 mg/kg) and xylazine (10 mg/kg). After a T9 laminectomy, a mid-thoracic SCI was produced using the IH injury device (Precision Systems and Instrumentation).[2] A previous study suggests that the duration of compression has negligible effects on outcomes.[11] Based on these findings, we performed pilot studies examining different compression times and found no obvious differences in injury severity between groups. This finding is consistent with a previous study reporting an injury threshold at 15 sec of sustained compression after IH contusion SCI.[9] Thus, we determined a 20 sec sustained compression was sufficient and reproducible within our stereotaxic mode of injury application.

Mice were divided randomly to receive SCI with varying impact force (50 or 75 kdyn) and duration of maintained compression (i.e., dwell time: 0 or 20 sec), yielding four groups: 50 kdyn, 50 kdyn 20 sec, 75 kdyn, and 75 kdyn 20 sec. After injury, muscle and skin incisions were closed using monofilament suture. Post-surgically, animals received one subcutaneous injection of buprenorphine-SR (1 mg/kg) for pain and 2 mL of saline + antibiotic (5 mg/kg, enroloxacin 2.27%: Norbook Inc, Lenexa, KS); buprenorphine has been shown to produce analgesic effects without affecting molecular, anatomical, behavior, or physiological parameters after SCI.[17]

Animals were housed in warming cages overnight. Animals continued to received 1 mL saline + prophylactic antibiotics subcutaneously for five days. Food and water intake and the incision site were monitored throughout the course of the study. Bladder expression was performed on injured mice twice daily until mice reached voluntary evacuation. Two mice received SCI with abnormalities in the force versus time curve generated by the IH device indicating bone contact or spinal cord movement during impact. Based on these pre-determined exclusion criteria, these two mice were excluded from further analyses.

Behavioral analysis

Locomotor hindlimb function was assessed using the BMS as described previously.[18] Two observers blinded to group inclusion observed and scored mice in an open field for 4 min at 1, 3, 7, 14, 21, and 28 days post-injury (dpi). Each hindlimb was scored separately based on movement (e.g., ankle placement and stepping), coordination, and trunk stability, then averaged to generate a single score for each animal. A score of 0 indicates complete paralysis while a score of 9 indicates normal locomotion. The BMS subscore is sensitive to atypical patterns of locomotor recovery[18] and was used to analyze specific aspects of locomotion (e.g., paw placement and coordination).

Tissue processing and histochemistry

At 3, 7, 14, or 28 dpi, mice were anesthetized with a lethal dose of ketamine (150 mg/kg) and xylazine (15 mg/kg), then transcardially perfused with cold phosphate buffered saline (PBS) (0.1 M, pH 7.4), followed by perfusion with cold 4% paraformaldehyde (PFA). Dissected spinal cords (1 cm) were post-fixed for 2 h in 4% PFA, then rinsed and stored in cold phosphate buffer (0.2 M, pH 7.4) overnight at 4°C. Tissue was cryoprotected in 30% sucrose at 4°C for one week, then rapidly frozen using optimal cutting temperature compound (Sakura Finetek USA, Inc., Torrance, CA) on dry ice. Tissue was systematically randomized into blocks with equal group distribution in each block to ensure uniformity of staining across groups. Tissue was stored at −80°C before sectioning. Tissue blocks were cut in serial cross sections (10 μm thick) and mounted onto Colorfrost plus slides (Fisher #12-550-17).

As validated and described previously, spared tissue was identified using a combination of eriochrome cyanine (EC) and neurofilament (NF) (Aves Labs, #NFH) to label myelin and axons, respectively.[19,20] For immunohistochemical analyses of macrophage phenotypes, sections were incubated with goat anti-CD206 (1:100

dilution, AF2535, R&D Systems, Minneapolis, MN), goat anti-Arg1 (1:100, SC-18354, Santa Cruz Biotechnology, Dallas, TX), rat anti-CD86 (1:100, 553689, BD Biosciences, San Jose, CA), or rat anti-MARCO (1:1000, MCA1849, BioRad, Hercules, CA). Slides were incubated with these primary antibodies overnight at 4°C in 0.1M PBS with 5% normal donkey serum, 0.1% fish gelatin (Sigma-Aldrich, G7765), 1% BSA and 0.1% Triton X-100. Sections were subsequently incubated with a biotinylated tomato lectin (1:1000, L0651; Sigma-Aldrich, St. Louis, MO) to counterstain for total macrophage numbers.

Detection of primary antibodies was performed with donkey anti-rat Alexa Fluor (AF) 488, donkey anti-rabbit AF 568, and streptavidin AF 647 (all secondaries at 1:1000 dilution, Life Technologies, Carlsbad, CA) for 1 h at room temperature. To validate antibody staining, negative controls were run without primary antibody, and full dilution curves were analyzed.

The EC/NF images were captured using an Olympus AX-80 and Aperio Scanscope. To quantify spared tissue, the regions of dense EC staining were outlined and measured using the MetaMorph analysis program (Molecular Devices, Sunnyvale, CA). To quantify macrophage activation, three or four regions of interest (ROI) were captured per subject using an Axioplan 2 imaging microscope (Carl Zeiss) at 20× magnification. The ROI were taken from within the lesion epicenter using NF/EC stained serial sections as references (Fig. 3A). Threshold based area measures of positive signal within the ROI were performed using MetaMorph to determine total area of positive signal. The total area of positive signal of macrophage markers (Arg1, CD206, MARCO, CD86) was then normalized to total tomato lectin (TomL) positive area for each ROI to determine proportion of positive macrophages within the lesion.

Because of unknown, at the time, temperature inconsistencies during tissue processing and sectioning, some cross sections were lost or folded during staining, making analysis impossible. Mice without an obvious and fully intact epicenter were not included for histological analysis, decreasing the total number of mice analyzed for histological analyses from 88 to 71.

Statistical analysis

Investigators blinded to experimental groups performed all data acquisition and analysis. Statistical analyses were completed using GraphPad Prism 6.0 (GraphPad Software). Data were analyzed using one- or two-way analysis of variance (ANOVA) followed by the Holm-Sidak test for multiple comparisons. Specifically, repeated measures two-way ANOVA was used to analyze BMS (time [repeated] × injury), 28 d tissue sparing (distance [repeated] × injury), and macrophage phenotype (ROI [repeated] × injury). Ordinary two-way ANOVA was used to analyze tissue sparing over time (time × injury). All other outcomes were analyzed using one-way ANOVA or independent sample *t* tests when appropriate.

Comparisons include groups differing only in contusion force (50 kdyn vs. 75 kdyn, 50 kdyn 20 sec vs. 75 kdyn 20 sec) or compression (50 kdyn vs. 50 kdyn 20 sec, 75 kdyn vs. 75 kdyn 20 sec); other groups were not analyzed statistically to avoid comparing across multiple independent variables. The robust regression and outlier removal method with a false positive rate for detecting outliers (Q-value) of 1% was used to automatically identify outliers, and imputed mean values were used when necessary for repeated measures.[21] Results were considered statistically significant at $p \leq 0.05$. All data are presented as mean ± standard error of the mean unless otherwise noted. Figures were prepared using Adobe Photoshop CS6 (Adobe Systems) and Prism 6.0.

Results

To understand the effects of compression at various contusion forces, we used the IH impactor to maintain spinal cord displacement after a controlled contusion. We have observed in pilot studies that injury variability can arise from the force-sampling rate of the IH device. To determine whether this variability affected tissue displacement and/or impact force across groups, we first quantified the tissue displacement and impact force during SCI across all groups. Tissue displacement and actual force were significantly different for 50 versus 75 kdyn injuries, regardless of compression ($p < 0.01$) (Table 1). Force-matched groups did not differ significantly in tissue displacement or actual force irrespective of compression ($p > 0.05$) (Table 1). These data indicate that compression did not alter force or displacement thus, differences in force-matched groups can be attributed solely to the addition of compression.

Table 1. Spinal Cord Injury Parameters

Group	*Set force (kdyn)*	*Actual force Avg. (kdyn) ± SD*	*Displacement Avg. (μm) ± SD*	*Compression time (s)*
50 kdyn	50	54 ± 2	429 ± 88	0
50 kdyn 20 sec	50	53 ± 2	398 ± 99	20
75 kdyn	75	78 ± 2	566 ± 99	0
75 kdyn 20 sec	75	78 ± 2	492 ± 76	20

SD, standard deviation.

Compression impairs functional recovery

To determine whether compression subsequent to contusion SCI alters functional recovery, we examined locomotor function in an open field using the BMS at 1, 3, 7, 14, 21, and 28 dpi. The BMS covers a wide range of functional recovery, from ankle movement to trunk and tail movements.[18] Consistent with previous reports,[3,18] locomotor function varied significantly depending on the contusion force; specifically, recovery was significantly worse for animals receiving 75 kdyn versus 50 kdyn contusions regardless of compression (main effect of 50 kdyn vs. 75 kdyn or 50 kdyn 20 sec vs. 75 kdyn 20 sec $p < 0.01$; Table 2 and Fig. 1). Compression also significantly decreased recovery independent of contusion severity (main effect of 50 kdyn vs. 50 kdyn 20 sec or 75 kdyn vs. 75 kdyn 20 sec $p < 0.0001$).

To account for atypical patterns of recovery that may occur with sustained compression, we further investigated recovery using the BMS subscore at 28 dpi. This composite score is based on the functional levels achieved for stepping, coordination, paw position, trunk stability, and tail placement independent of the pattern, or progression, of recovery.[18] Figure 1B shows that the total BMS subscore is decreased by increased contusion force (50 kdyn vs. 75

Table 2. Basso Mouse Scale Significance

Groups (n)	*Main*	*1 dpi*	*3 dpi*	*7dpi*	*14 dpi*	*21 dpi*	*28 dpi*
50 kdyn ($n = 11$) vs. 75 kdyn ($n = 9$)	**	0.14	0.27	***	0.09	*	*
50 kdyn 20 sec ($n = 9$) vs. 75 kdyn 20 sec ($n = 10$)	***	0.65	0.92	0.07	***	****	****
50 kdyn ($n = 11$) vs. 50 kdyn 20 sec ($n = 10$)	****	*	**	****	***	****	****
'75 kdyn ($n = 9$) vs. 75 kdyn 20 sec (n = 10)	****	0.78	0.27	***	****	****	****

*,**,***,**** $p < 0.05$, 0.01, 0.001, 0.0001.

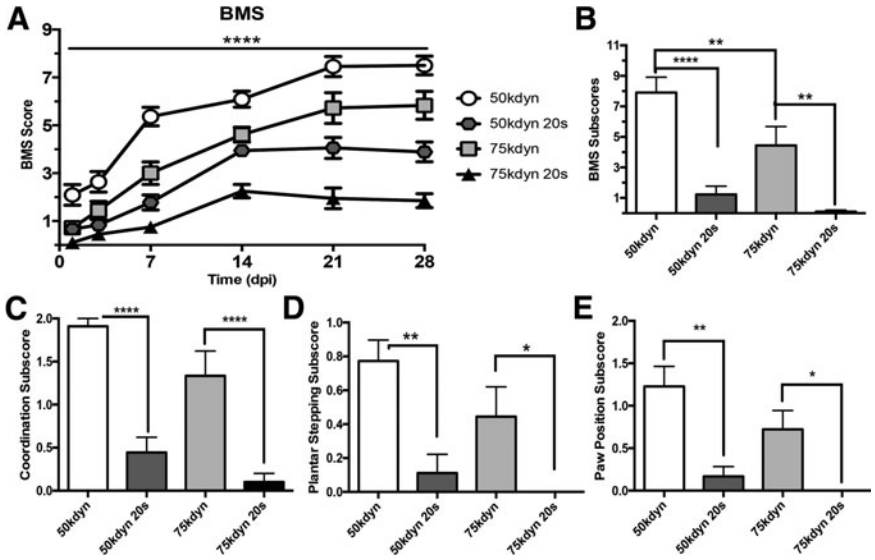

FIG. 1. Compression impairs functional recovery from contusion spinal cord injury. Time course of locomotor recovery assessed by Basso Mouse Scale (**A**) and BMS subscore (**B–E**). (A) Over a 28-day period, groups with increased impact force score lower than groups with decreased impact force and groups with compression score lower than noncompression groups. Significance between comparable groups at each time point is detailed in Table 2 ($n = 9–11$; mean ± standard error of the mean [SEM]). (B–E) 28 dpi BMS subscores ($n = 9–11$). (B) Composite BMS subscore is significantly different between compression and noncompression groups. (C) Coordination is graded as 2 = mostly coordinated (>50%), 1 = some coordination (<50%), or 0 = no coordination. (D) Plantar stepping is graded as 1 = consistent or 0 = less than consistent. (E) Paw position is graded as 2 = parallel throughout, 1 = parallel and rotated, or 0 = rotated throughout. Groups with compression performed significantly worse than force-matched counterparts for every subscore. B–E: ****$p < 0.0001$, **0.01, *0.05. Mean ± SEM.

kdyn, $p < 0.05$), and with the addition of compression at each contusion force (50 kdyn vs. 50 kdyn 20 sec, $p < 0.0001$; 75 kdyn vs. 75 kdyn 20 sec, $p < 0.01$). Particular aspects of the BMS subscore highlight specific functional tasks, all of which follow a similar pattern to the overall BMS subscore and functional outcomes at 28 dpi.

Figure 1C shows the coordination subscore that quantifies forelimb-hindlimb stepping as mostly coordinated (≥50% coordination, score = 2), some coordination (≥1 coordinated pass, score = 1), or no coordination (score = 0). Compression significantly decreased forelimb-hindlimb stepping coordination (50 kdyn vs. 50 kdyn 20 sec, $p < 0.0001$; 75 kdyn vs. 75 kdyn 20 sec, $p < 0.0001$). Figure 1D shows the plantar stepping subscore that distinguishes between frequent hindlimb plantar stepping (≥50% stepping, score = 1) and occasional/no hindlimb plantar stepping (<50% stepping, score = 0). Compression significantly decreased hindlimb plantar stepping performance (50 kdyn vs. 50 kdyn 20 sec, $p < 0.01$; 75 kdyn vs. 75 kdyn 20 sec, $p < 0.05$).

Figure 1E shows the paw position subscore, which quantifies paw rotation during stepping from the initial contact through liftoff as parallel throughout (score = 2), parallel and rotated (score = 1), or rotated throughout (score = 0). Compression significantly worsened paw positioning during stepping (50 kdyn vs. 50 kdyn 20 sec, $p < 0.001$; 75 kdyn vs. 75 kdyn 20 sec, $p < 0.05$) Collectively, BMS score and subscore indicate that functional recovery is impaired by additional compression at the time of contusion regardless of impact force.

Compression impairs anatomical recovery

To determine whether long-term anatomical recovery was affected by the addition of compression to a contusion SCI, we next investigated tissue changes through histological analysis of serial spinal cord cross sections. We performed tissue-sparing analysis at 28 dpi using EC and NF staining on sections 0.2 mm, 0.5 mm, and 1.0 mm rostral and caudal to the lesion epicenter. As reported previously,[3] epicenter tissue sparing decreased with impact force (50 kdyn vs. 75 kdyn $p = 0.03$; Fig. 2A and Table 3). Similar to our findings with functional recovery, compression significantly decreased tissue sparing regardless of impact force at the lesion epicenter (50 kdyn vs. 50 kdyn 20 sec and 75 kdyn vs. 75 kdyn 20 sec $p < 0.0001$) and up to 1 mm rostral and caudal to the epicenter (Fig. 2A and Table 3).

To gain insight into the progression of tissue damage, additional epicenter tissue sparing data were gathered at 3, 7, and 14 dpi. While the amount of spared tissue changes over this period (likely because of tissue edema and changes in myelin breakdown and clearance), we observed compression caused long-term spared tissue loss relative to contusion alone (Fig. 2B and Table 4).

Compression alters SCI macrophage phenotype

We began to observe significant compression-mediated differences in tissue sparing and functional recovery at seven days after injury with a clear plateau by 14 dpi. These time points coincide with the peak of SCI macrophage infiltration and subsequent predominance of proinflammatory macrophage activation.[13,22] Because different macrophages phenotypes can promote tissue recovery or exacerbate neuronal death, we looked at established markers for macrophage polarization in response to different impact forces and added compression at 7 and 14 dpi. CD206 and Arg1 detect alternatively activated, potentially reparative macrophages (M2), and CD86 and MARCO detect classically activated,

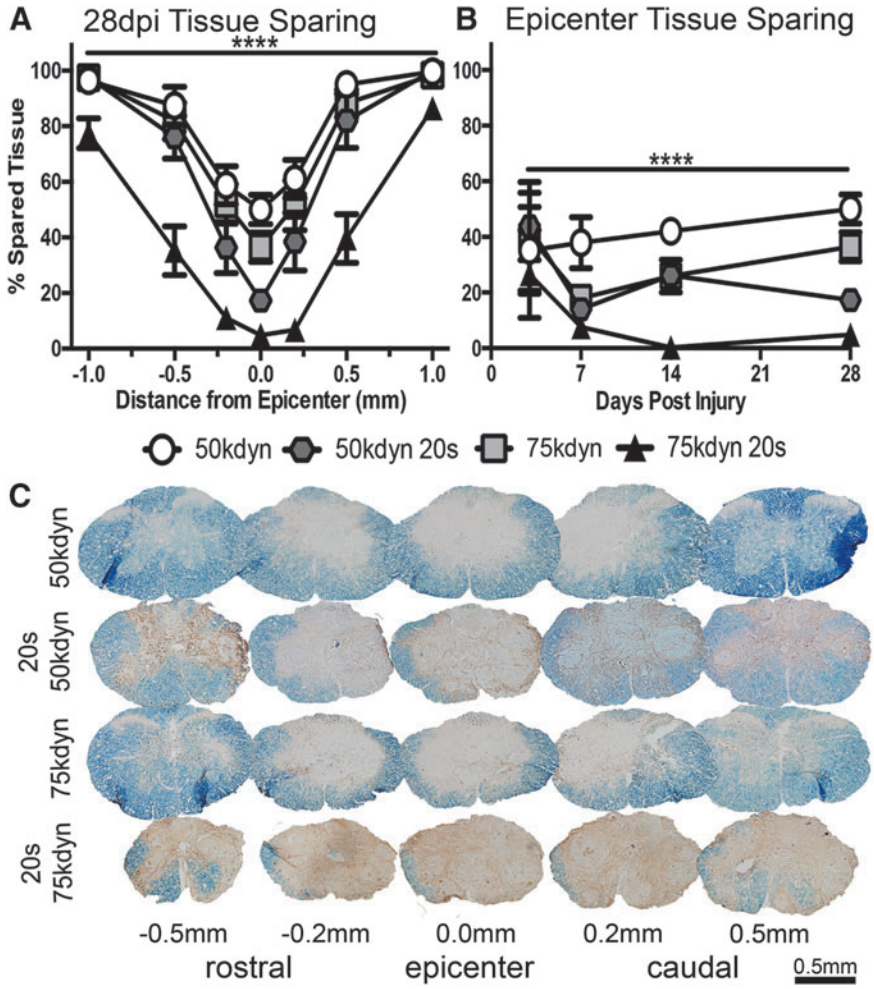

FIG. 2. Compression significantly decreases anatomical recovery from contusion spinal cord injury. (**A**) Tissue sparing at 28 dpi is decreased by both increased force and compression at the epicenter and at regions rostral and caudal to the epicenter ($n = 8$–9, mean ± standard error of the mean [SEM]). (**B**) Tissue sparing at 3, 7, 14, and 28 dpi, reflected by eriochrome cyanine (EC) for myelin and neurofilament (NF) for axons, at the lesion epicenter is decreased by both increased impact force and compression (3 dpi $n = 2$–4, 7 dpi $n = 3$, 14 dpi $n = 5$, 28 dpi $n = 8$–9, mean ± SEM). (**C**) Sections, representative of the mean of each group, reflect decreased tissue sparing in groups that receive compression. EC (blue), NF (brown) Scale bar, 400 μm. ****Significance for compared groups detailed in Table 3.

cytotoxic macrophages (M1) (see supplementary Fig. 1; see online supplementary material at ftp.liebertpub.com).[15,23]

To quantify macrophage infiltration while controlling for potential differences in lesion severity, we determined the macrophage density using three to four areas (ROI) within the lesion epicenter (Fig. 3A). Although lesion size varied across groups, we observed a similar macrophage density within the lesion epicenter in all injury groups at both time points (Fig. 3A and Fig. 4A, $p > 0.4$; main effect injury, $n = 3$–5).

At 7 dpi, there was no effect of force or compression on the percentage of macrophages positive for protective markers, CD206 ($p = 0.4$ and 0.6, main effect of force and compression, respectively) and Arg1 ($p = 0.7$ and 0.5, main effect of force and compression, respectively) (Fig. 3B,C). Similarly, macrophages positive for the proinflammatory marker, CD86, are present at comparable levels with a force-dependent trend toward increased expression after 50 kydn injuries ($p = 0.1$ and 0.5, main effect of force and compression, respectively, Fig. 3D). We observed a significant difference,

Table 3. Tissue Sparing Significance

		Rostral (mm)			*Epicenter*	*Caudal (mm)*		
Groups (n)	*Main*	*1*	*0.5*	*0.2*	*0*	*0.2*	*0.5*	*1*
50 kdyn ($n = 8$) vs. 75 kdyn ($n = 9$)	0.28	>0.99	0.99	0.97	0.46	0.84	0.97	>0.99
50 kdyn 20 sec ($n = 8$) vs. 75 kdyn 20 sec ($n = 9$)	***	0.16	****	*	0.72	**	***	0.63
50 kdyn ($n = 8$) vs.50 kdyn 20 sec ($n = 8$)	**	>0.99	0.78	0.08	**	0.07	0.48	>0.99
75 kdyn ($n = 9$) vs.75 kdyn 20 sec ($n = 9$)	****	0.10	****	****	**	****	****	0.65

*,**,***,**** $p < 0.05$, 0.01, 0.001, 0.0001.

Table 4. Tissue Sparing Time Course

	p *value*				
Groups	*Main*	*3 dpi* (n = *2–4*)	*7 dpi* (n = *3*)	*14 dpi* (n = *5*)	*28 dpi* (n = *8–9*)
50 kdyn vs. 75 kdyn	**	0.99	0.29	0.25	0.18
50 kdyn 20 sec vs. 75 kdyn 20 sec	****	0.52	0.74	****	**
50 kdyn vs. 50 kdyn 20 sec	****	0.90	0.07	0.16	****
75 kdyn vs. 75 kdyn 20 sec	****	0.58	0.60	***	****

*,**,***,**** $p < 0.05$, 0.01, 0.001, 0.0001.

however, in the percent of macrophage positive for MARCO (Fig. 3E,F) with compression at the time of contusion increasing the proportion of MARCO+ cells twofold to threefold compared with contusion alone (50 kdyn 20 sec = 10.3% and 75 kdyn 20 sec = 14.0% vs. 50 kdyn = 2.4% and 75 kdyn = 3.6%; main effect of compression $p = 0.02$, main effect of force $p = 0.5$).

At 14 dpi, we observed that compression at the time of contusion decreased the proportion of Arg1+ macrophages one and one half to twofold compared with contusion alone (50 kdyn 20 sec = 13.0% and 75 kdyn 20 sec = 17.8% vs. 50 kdyn = 23.8% and 75 kdyn = 29.05%; main effect of compression $p = 0.04$, main effect of force, p = 0.4) (Fig. 4B,C). We observed no effect of injury type on the percentage of macrophages positive for CD206 ($p = 0.3$ and $p = 0.5$, main effect force and compression, respectively; Fig. 4D) or CD86 ($p = 0.3$ and $p = 0.3$; main effect force and compression, respectively; Fig. 4E). In addition, whereas MARCO staining was observed on the cell surface of macrophages cells at 7 dpi (Fig. 3E), by 14 dpi, MARCO displayed fractured staining with no definitive localization in all treatment samples (Supplementary Fig. 1; see online supplementary material at ftp.liebertpub.com). Thus, we did not observe any MARCO+/TomL+ cells at 14 dpi. Collectively, we conclude from these data that compression alters the inflammatory environment of the injured spinal cord.

The effects of compression are independent of injury severity

The effects of compression we observed between 75 kdyn versus 75 kdyn 20 sec and 50 kdyn versus 50 kdyn 20 sec could be because of increased injury severity or the inherent properties of subsequent compression SCI. To determine the effect of compression independent of contusion force and injury severity, we collapsed across 50 and 75 kdyn SCI groups to compare contusion alone with contusion with 20 sec compression. Functional ability, according to BMS, is significantly decreased by the addition of compression at all time points (Fig. 5A; $p < 0.0001$, main effect of compression). Specifically, functional recovery is impaired by the addition of compression; mice that did not receive sustained compression improved, on average, 1.5 points on the BMS scale between 14 dpi and 28 dpi (Fig. 5A,B). On the other hand, mice receiving sustained compression after contusion SCI improve significantly less ($p < 0.005$), on average 0.3 points on the BMS scale (Fig. 5B).

Similarly, anatomical recovery, quantified by tissue sparing at the lesion epicenter, is significantly decreased with the addition of compression ($p < 0.001$ main effect of compression) with effects evident by 14 dpi (Fig. 5C). In addition, compression significantly increased MARCO expression and decreased Arg1 expression on SCI macrophages (Fig. 5D main effect of compression $p < 0.05$). These data show that compression across contusion forces, regardless of injury severity, has significant effects on the secondary injury responses, functional recovery, and inflammation after contusion SCI.

Discussion

Clinical SCI has highly variable modes of injury, including interactions of biomechanics such as compression and contusion. In this study, we examined how the initial mode of impact affects functional recovery, anatomical recovery, and inflammation. Specifically, our investigation into the differences in contusion injury at variable forces with and without compression yielded three major findings: compression after contusion SCI (1) decreases functional recovery and affects recovery progression, (2) decreases anatomical recovery and tissue sparing, and (3) drives increased proinflammatory (M1) macrophage activation. Collectively, these observations strongly support the overall concept that the biomechanics of injury affect secondary injury progression and highlight the potential for the efficacy of immunomodulatory therapies to be injury dependent.

In the current study, we observed a compression-dependent decrease in anatomical recovery over time regardless of the initial contusion force. This is consistent with reports of altered perfusion, energy metabolism, hemorrhage, and revascularization with compression after contusion SCI.[8,10,24] Notably, compression induces increased hemorrhage, decreases spinal cord perfusion, and increases indicators of hypoxia in penumbral and distal areas of the spinal cord relative to the lesion epicenter.[8,10,24] These areas are often spared from the initial mechanical damage and are most susceptible to secondary injury.

Any biomechanical-specific changes in secondary injury mechanisms in these areas are likely to manifest as alterations in functional recovery. Independent of the magnitude of SCI contusion, we noted that subsequent compression significantly decreases both functional and anatomical recovery. Specifically, locomotor recovery ceased two weeks after combined contusion and compression injury with a coincident plateau of anatomical recovery. Interestingly a similar two-week plateau in functional recovery has been reported after varying degrees of compression injury alone and after severe IH contusion injury.[3,25] While it is not surprising that little recovery would be detectable after severe injuries, it is interesting to note that clip-compression SCI, a form of contusion with sustained compression, results in little recovery after the first few weeks of injury in both rats and mice.[5,26]

Only a few studies have reported long-term recovery after contusion injury with or without subsequent compression. For example, Streijger and colleagues[9] examined fore and hindlimb recovery after cervical IH contusion in mice with or with subsequent compression (0, 15, or 30 sec). Depending on the outcome measure, recovery was noted in the contusion alone group after two weeks (e.g., forelimb grip strength); however, little recovery was observed within the first month across a range of functional measures in combined contusion-compression groups.[9] Chronically (12 wks), some behaviors did improve across all groups; however, functional decline was noted only in the combined contusion/compression groups over this period.

The behavioral results are less consistent in rat models of contusion with subsequent compression injury. When a spacer was

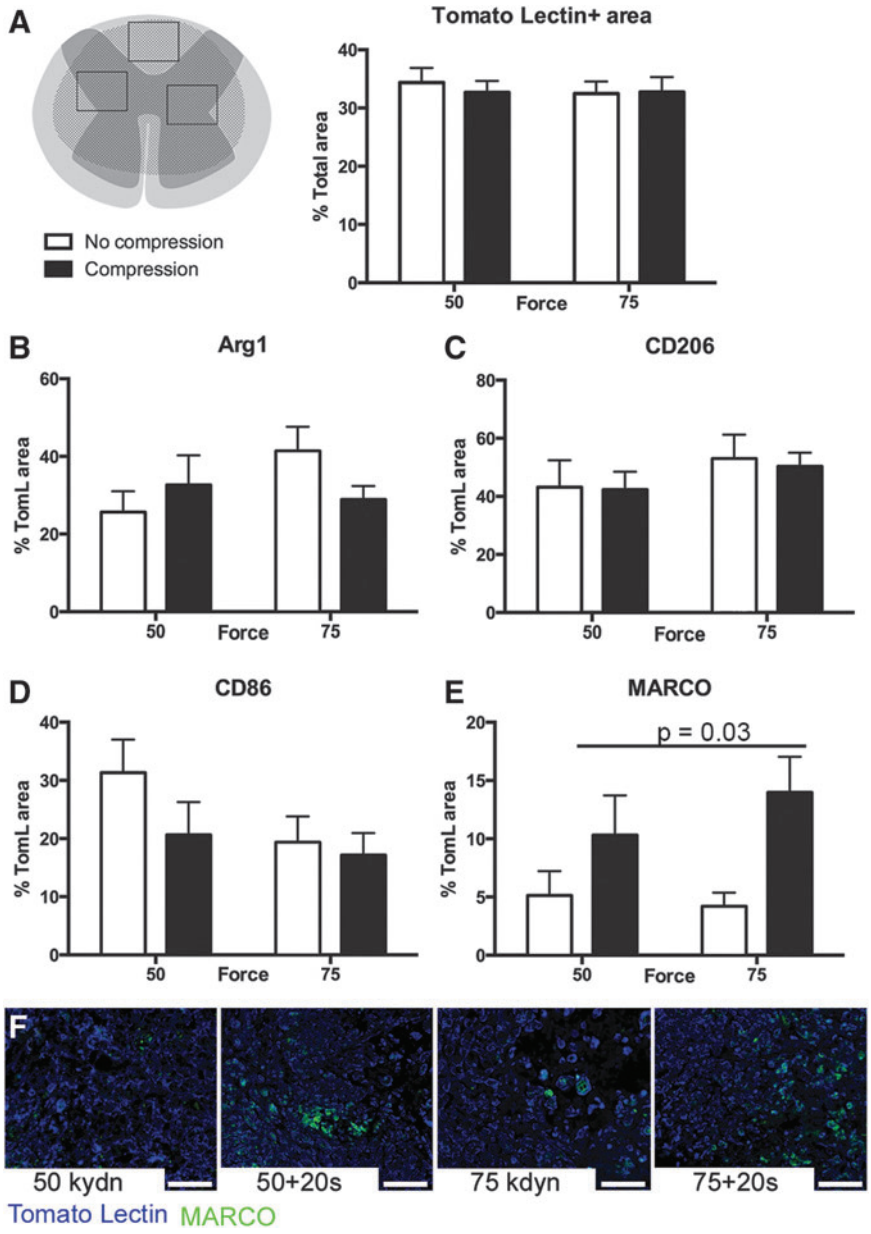

FIG. 3. Compression alters spinal cord injury macrophage activation at 7 dpi. (**A**) Three regions of interest (ROI; dorsal and left and right) within the lesion epicenter of each animal were analyzed at 7 dpi for macrophage density (total tomato lectin [TomL] positive area). The TomL + area was similar across the four injury paradigms: 50 kdyn, 75 kdyn without compression (open bars) and 50 kdyn, 75 kdyn with compression (black bars). (**B**) Percent of TomL+ cells positive for Arginase 1 (Arg1) across treatments. (**C**) Percent of TomL+ cells positive for CD206 across treatments. (**D**) Percent of TomL+ cells positive for CD86, and (**E**) percent of TomL+ cells positive for macrophage receptor with collagenous structure (MARCO) ($p = 0.03$ main effect of compression). B–E) $n = 3$–4, error bars = SEM). (**F**) Representative images for analysis of Tomato lectin+ (blue)/MARCO+ (green) cells across treatments. Scale bar = 50 μm.

placed on the dura after contusion SCI to maintain compression for various periods (h to wks), the rate and overall extent of recovery varied with spacer size and compression duration.[12,24] These data, along with a rat study with various compression times after IH contusion,[11] indicate that the compression itself, and not the duration of the compression, worsens functional outcome. Collectively, these published results, along with the results of the current study, indicate that the mode of injury is an important determinant of functional recovery. Indeed, a recent comparison across contusion, dislocation, and distraction SCI reported different rates of recovery depending on the mode of SCI.[27]

Because we noted decreased tissue and functional recovery in groups receiving compression regardless of the contusion force, this suggests that the injury mode, and not just overall injury severity itself, may be an important determinant of secondary injury environment. This is consistent with previous observations of secondary pathology across different types of SCI[1,28] and is supported by our previous observation that the efficacy of neuroprotective SCI therapies is dependent on the mode and biomechanics of the initial injury.[29]

Neuroinflammation plays a major role in orchestrating secondary injury mechanisms (reviewed in [15]). Specifically, macrophage

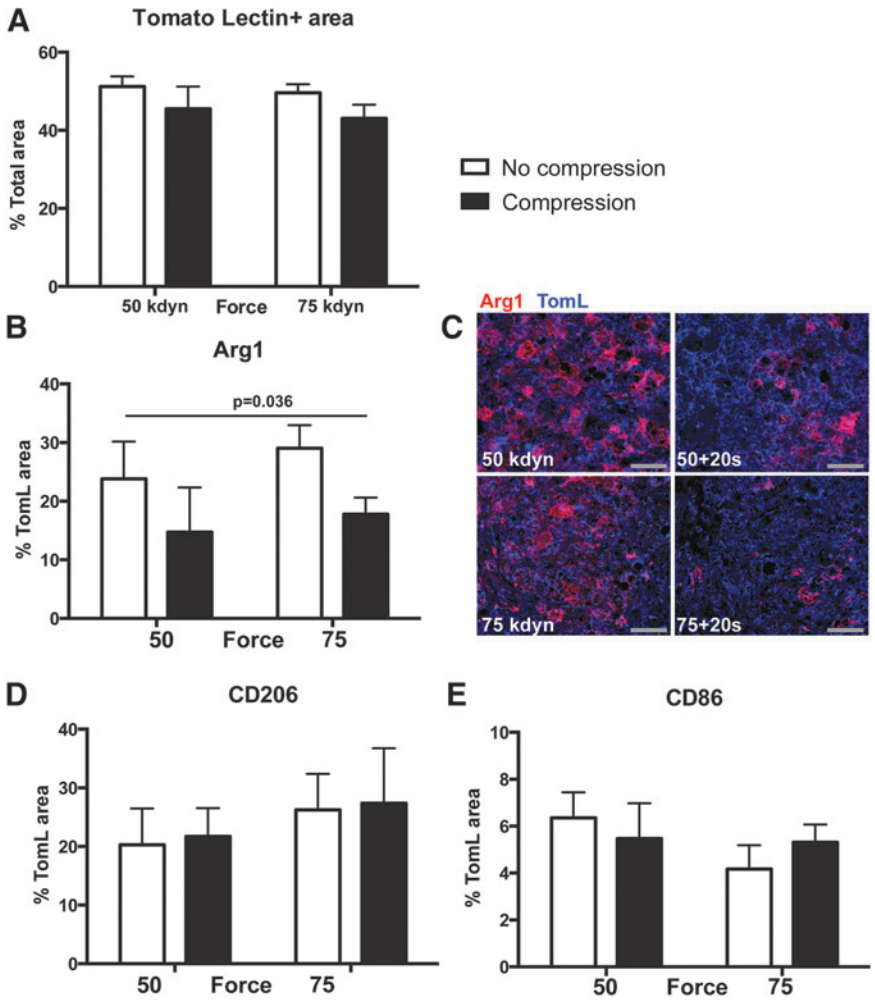

FIG. 4. Compression alters spinal cord injury macrophage activation at 14 dpi. (**A**) Four regions of interest within the lesion epicenter of each animal (as depicted in Fig. 3A and ventral) were analyzed at 14 dpi for macrophage density (total tomato lectin [TomL] positive area). The TomL + area was comparable across all four injuries: 50 kdyn, 75 kdyn without compression (open bars) and 50 kdyn, 75 kdyn with compression (black bars). (**B**) Percent of TomL+ cells positive for Arginase 1 (Arg1) across treatments ($p = 0.036$ main effect compression). (**C**) Representative images for analysis of tomato lectin + (blue)/Arg1+ (red) cells across treatments. Scale bar = 50 μm. (**D**) Percent of TomL+ cells positive for CD206, and (**E**) percent of TomL+ cells positive for CD86. $n = 5$, error bars = standard error of the mean.

activation is dictated, in part, by the microenvironment, and macrophages can adopt proinflammatory, neurotoxical phenotypes or purportedly reparative phenotypes depending on the stimuli present in the injured spinal cord.[13] A novel observation in the current study is that the proportion of macrophages expressing markers indicative of a pathological phenotype increased with a decrease in markers indicative of a reparative phenotype with compression after the contusion injury. It is important to note that we normalized to the overall magnitude of the macrophage response, thereby concluding that biomechanics, and not injury severity alone, may be an important driver of macrophage activation after SCI.

In support of this idea, it was observed previously that the extent of microglial/macrophage activation after SCI varied across contusion, dislocation, and distraction injuries.[1] Differences also have been observed in the immune system response to brain versus SCI.[30] Indeed, while both central nervous system organs are extremely similar, subtle differences in blood barriers and resident glial cells can lead to robust differences in immune cell activity and distribution.[31,32] In addition, Zhang and associates[33] show convincingly microenvironment-specific differences in toll-like receptor 4 (TLR4) expression on activated macrophages after compression SCI. TLR4 is important for lipopolysaccharide-mediated proinflammatory macrophage activation, and that article demonstrated that even within the same organ with the same injury, microenvironmental conditions significantly impact proinflammatory responses.

It is also important to consider that although microglia and monocyte-derived macrophages express similar histological markers of myeloid cells, they are distinct populations and may play distinct roles in SCI pathophysiology. We observed compression-specific changes in MARCO and Arg1. Interestingly, both of these phenotypic markers are predominantly expressed in monocyte-derived macrophages. Specifically, using a transgenic model to label infiltrating cells, Greenhalgh and coworkers[34] detected Arg1 exclusively on monocyte-derived macrophages after contusion SCI.

Targeting MARCO reduces monocyte trafficking in models of myocardial infarction, experimental autoimmune encephalomyelitis,

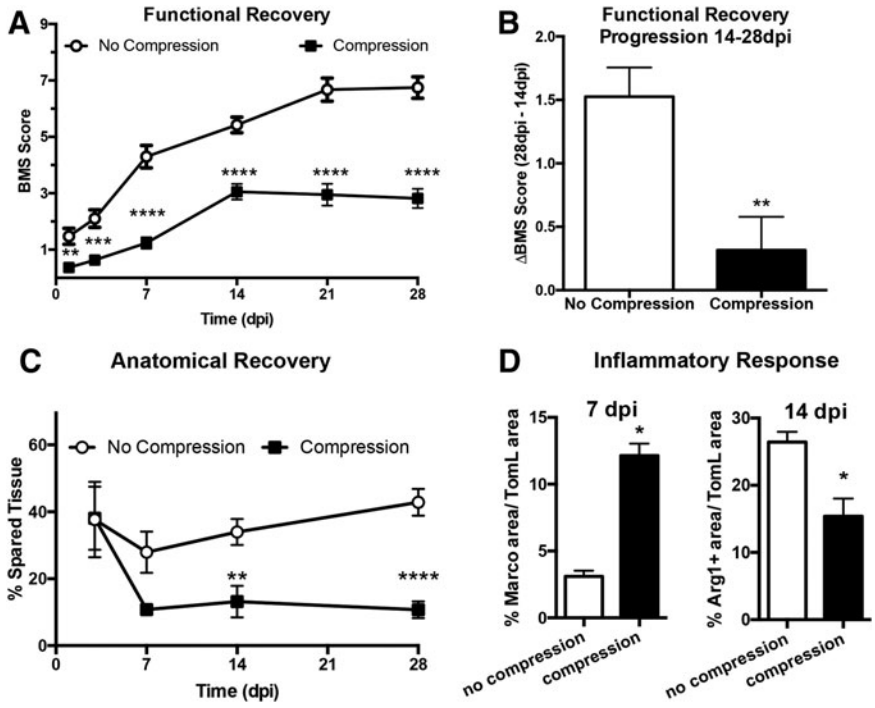

FIG. 5. Compression decreases functional recovery, anatomical recovery, and alters inflammatory macrophage profile regardless of contusion severity. Both 50 and 75 kydn spinal cord injury contusion groups were collapsed and the effect of 20s of sustained compression compared between aggregate groups. (**A**) Animals with compression injuries perform worse, according to the Basso Mouse Scale, at all time points than noncompression injury counterparts ($n = 19$–20). In addition, (**B**) noncompression injured animals demonstrate improved function from 14 to 28 dpi, while compression injured animals have stunted recovery after 14 dpi ($n = 19$–20). (**C**) Tissue sparing at the lesion epicenter, determined by eriochrome cyanin for myelin and neurofilament for axons, significantly decreases by 14 dpi with the addition of compression (3 dpi $n = 6$, 7 dpi $n = 6$, 14 dpi $n = 10$, 28 dpi $n = 17$). (**D**) Tomato lectin-labeled macrophages increase expression of the pro-inflammatory marker, macrophage receptor with collagenous structure (MARCO) ($n = 6$) and decrease Arginase 1 expression ($n = 10$). ****$p < 0.0001$, ***$p < 0.001$, **$p < 0.01$, *$p < 0.05$, data are mean ± standard error of the mean. BMS, Basso Mouse Scale.

colitis, peritonitis, and encephalitis[35]; therefore, MARCO may be a hallmark for proinflammatory monocytes. Indeed, in the current study, we focused our analyses on the lesion core, an area predominantly populated by monocyte-derived macrophages after contusion SCI.[36] Collectively, our observations suggest that compression polarizes monocyte-derived macrophages toward a proinflammatory phenotype. It is also possible the compression alters the distribution of microglia after injury or upregulates markers in microglia not normally expressed after contusion SCI. Further studies are warranted to parse out the specific contribution of injury biomechanics to environmental and chemotactic cues for macrophages and microglia independently.

In the current study, we detected a compression-specific increase in the proportion of macrophages expressing MARCO. MARCO is a class A scavenger receptor that assists in the phagocytosis of a wide variety of particles and promotes production of proinflammatory cytokines mediated through TLR2 signaling.[37,38] The binding properties of MARCO enable this cell surface receptor to recognize pathogen- and damage-associated molecular patterns with polyanionical properties. Specifically, MARCO can recognize lipopolysaccharides, nucleic acids, and modified lipids,[39–41] and the loss of macrophage-specific MARCO expression leads to accumulation of oxidized lipids in lung models of oxidant inhalation.[42] Interestingly, the mode of SCI influences microenvironmental factors such as 3-NT, cytochrome c, and membrane permeability.[1,28] Compression, specifically, adds a component of reperfusion and hemorrhage that alters fluid dynamics.[5,8,43] Collectively, these published data and the increased MARCO+ macrophages observed with compression in the current study, indicate increased damage caused by reperfusion, excessive oxidants and oxidized lipids with compression in contusion SCI.

The shift in MARCO and Arg1 cells not only reflects differences in the microenvironment after a compression-contusion injury, but also is a likely player in secondary pathology. MARCO is specifically expressed by proinflammatory, neurotoxical M1 macrophages[23] and is integral in the uptake of immune-modifying microparticles, which subsequently inhibits trafficking of pathological macrophages.[35] Previously we observed an age-dependent decrease in recovery and increased tissue pathology coincident with decreased macrophage Arg1 expression.[44] Whether MARCO and Arg1 alone or a large repertoire of proteins are affected by the compression microenvironment, these secondary responses are likely critical to overall outcomes of SCI, and thus are important targets for therapeutic intervention.

The heterogeneous nature of human SCI creates a challenge for recapitulation in controlled experimental models. Resolving SCI into its composite parts has provided valuable insight. Extrapolation to clinical relevance, however, requires combinatorial approaches to avoid erroneous inductive generalizations. The model employed in this study provides valuable information about the interaction of biomechanics common to clinical SCI. It shows that compression affects overall outcomes, as well as at least one

secondary response to injury. This introduces a multitude of questions outside the scope of this study regarding the wide variety of secondary responses possibly affected by contusion, compression, or other biomechanics. Interestingly, emerging data also indicate that physiological factors such as age and sex impact secondary injury progression.[45–47] This merits further investigation into the biomechanical and physiological influences on the secondary response to SCI.

Conclusion

To more fully understand the effects of injury biomechanics and their interactions, we created a mouse model of contusion SCI that incorporates compression. This study reveals that compression decreases anatomical recovery and functional recovery regardless of contusion severity and affects recovery progression and macrophage activation. The premature cessation of functional recovery is likely because of changes in secondary responses caused by the addition of compression.

One potential player in this secondary response is inflammation. We observed compression-specific increase of at least one proinflammatory macrophage receptor, MARCO, followed by a subsequent decrease in Arg1, a marker of a reparative macrophage phenotype. This supports MARCO as an important and sensitive proinflammatory macrophage marker and highlights the importance of continued study of the effects of primary injury biomechanics on secondary responses and overall outcomes of SCI. Through continued studies of initial injury influences on secondary responses, clinicians and researchers will benefit in deeper understanding of model translation to the heterogeneous cases of human SCI.

Acknowledgments

This work was supported by NIH NINDS R01NS091582 and P30 NS051220; a University of Kentucky Postdoctoral Fellowship; the Craig H. Neilsen Foundation; the Math, Science, and Technology Center at Paul Laurence Dunbar High School; the Kentucky Spinal Cord and Head Injury Research Trust (support for BZ); and the Spinal Cord and Brain Injury Research Center at the University of Kentucky. We would like to thank Taylor Otto, Linda Zimmerman, and Ashley Seifert for their support.

Author Disclosure Statement

No competing financial interests exist.

References

1. Choo, A.M., Liu, J., Dvorak, M., Tetzlaff, W., and Oxland, T.R. (2008). Secondary pathology following contusion, dislocation, and distraction spinal cord injuries. Exp. Neurol. 212, 490–506.
2. Scheff, S.W., Rabchevsky, A.G., Fugaccia, I., Main, J.A., and Lumpp, J.E. Jr. (2003). Experimental modeling of spinal cord injury: characterization of a force-defined injury device. J. Neurotrauma 20, 179–193.
3. Ghasemlou, N., Kerr, B.J., and David, S. (2005). Tissue displacement and impact force are important contributors to outcome after spinal cord contusion injury. Exp. Neurol. 196, 9–17.
4. McEwen, M.L., and Springer, J.E. (2006). Quantification of locomotor recovery following spinal cord contusion in adult rats. J. Neurotrauma 23, 1632–1653.
5. Forgione, N., Karadimas, S.K., Foltz, W.D., Satkunendrarajah, K., Lip, A., and Fehlings, M.G. (2014). Bilateral contusion-compression model of incomplete traumatic cervical spinal cord injury. J. Neurotrauma 31, 1776–1788.
6. Huang, W.L., George, K.J., Ibba, V., Liu, M.C., Averill, S., Quartu, M., Hamlyn, P.J., and Priestley, J.V. (2007). The characteristics of neuronal injury in a static compression model of spinal cord injury in adult rats. Eur. J. Neurosci. 25, 362–372.
7. Gruner, J.A., Yee, A.K., and Blight, A.R. (1996). Histological and functional evaluation of experimental spinal cord injury: evidence of a stepwise response to graded compression. Brain Res. 729, 90–101.
8. Sjovold, S.G., Mattucci, S.F., Choo, A.M., Liu, J., Dvorak, M.F., Kwon, B.K., Tetzlaff, W., and Oxland, T.R. (2013). Histological effects of residual compression sustained for 60 minutes at different depths in a novel rat spinal cord injury contusion model. J. Neurotrauma 30, 1374–1384.
9. Streijger, F., Beernink, T.M.J., Lee, J.H., Bhatnagar, T., Park, S., Kwon, B.K., and Tetzlaff, W. (2013). Characterization of a cervical spinal cord hemicontusion injury in mice using the infinite horizon impactor. J. Neurotrauma 30, 869–883.
10. Okon, E.B., Streijger, F., Lee, J.H., Anderson, L.M., Russell, A.K., and Kwon, B.K. (2013). Intraparenchymal microdialysis after acute spinal cord injury reveals differential metabolic responses to contusive versus compressive mechanisms of injury. J. Neurotrauma 30, 1564–1576.
11. Swartz, K.R., Scheff, N.N., Roberts, K.N., and Fee, D.B. (2009). Exacerbation of spinal cord injury due to static compression occurring early after onset. J. Neurosurg. Spine 11, 570–574.
12. Dimar, J.R., Glassman, S.D., Raque, G.H., Zhang, Y.P., and Shields, C.B. (1999). The influence of spinal canal narrowing and timing of decompression on neurologic recovery after spinal cord contusion in a rat model. Spine 24, 1623–1633.
13. Kigerl, K.A., Gensel, J.C., Ankeny, D.P., Alexander, J.K., Donnelly, D.J., and Popovich, P.G. (2009). Identification of two distinct macrophage subsets with divergent effects causing either neurotoxicity or regeneration in the injured mouse spinal cord. J. Neurosci. 29, 13435–13444.
14. David, S., and Kroner, A. (2011). Repertoire of microglial and macrophage responses after spinal cord injury. Nat. Rev. Neurosci. 12, 388–399.
15. Gensel, J.C., and Zhang, B. (2015). Macrophage activation and its role in repair and pathology after spinal cord injury. Brain Res. 1619, 1–11.
16. Gensel, J.C., Donnelly, D.J., and Popovich, P.G. (2011). Spinal cord injury therapies in humans: an overview of current clinical trials and their potential effects on intrinsic CNS macrophages. Expert Opin. Ther. Targets 15, 505–518.
17. Santiago, J.M., Rosas, O., Torrado, A.I., González, M.M., Kalyan-Masih, P.O., and Miranda, J.D. (2009). Molecular, anatomical, physiological, and behavioral studies of rats treated with buprenorphine after spinal cord injury. J. Neurotrauma 26, 1783–1793.
18. Basso, D.M., Fisher, L.C., Anderson, A.J., Jakeman, L.B., Mctigue, D.M., and Popovich, P.G. (2006). Basso Mouse Scale for locomotion detects differences in recovery after spinal cord injury in five common mouse strains. J. Neurotrauma 23, 635–659.
19. Rabchevsky, A.G., Fugaccia, I., Sullivan, P.G., and Scheff, S.W. (2001). Cyclosporin A treatment following spinal cord injury to the rat: behavioral effects and stereological assessment of tissue sparing. J. Neurotrauma 18, 513–522.
20. Zhang, B., Bailey, W.M., Kopper, T.J., Orr, M.B., Feola, D.J., and Gensel, J.C. (2015). Azithromycin drives alternative macrophage activation and improves recovery and tissue sparing in contusion spinal cord injury. J. Neuroinflammation 12, 218.
21. Motulsky, H.J., and Brown, R.E. (2006). Detecting outliers when fitting data with nonlinear regression—a new method based on robust nonlinear regression and the false discovery rate. BMC Bioinformatics 7, 123.
22. Kigerl, K.A., McGaughy, V.M., and Popovich, P.G. (2006). Comparative analysis of lesion development and intraspinal inflammation in four strains of mice following spinal contusion injury. J. Comp. Neurol. 494, 578–594.
23. Gensel, J.C., Kopper, T.J., Zhang, B., Orr, M.B., and Bailey, W.M. (2017). Predictive screening of M1 and M2 macrophages reveals the immunomodulatory effectiveness of post spinal cord injury azithromycin treatment. Sci. Rep. 7, 40144.
24. Kubota, K., Saiwai, H., Kumamaru, H., Kobayakawa, K., Maeda, T., Matsumoto, Y., Harimaya, K., Iwamoto, Y., and Okada, S. (2012). Neurological recovery is impaired by concurrent but not by asymptomatic pre-existing spinal cord compression after traumatic spinal cord injury. Spine 37, 1448–1455.

25. Ropper, A.E., Zeng, X., Anderson, J.E., Yu, D., Han, I., Haragopal, H., and Teng, Y.D. (2015). An efficient device to experimentally model compression injury of mammalian spinal cord. Exp. Neurol. 271, 515–523.
26. Joshi, M., and Fehlings, M.G. (2002). Development and characterization of a novel, graded model of clip compressive spinal cord injury in the mouse: Part 1. Clip design, behavioral outcomes, and histopathology. J. Neurotrauma 19, 175–190.
27. Chen, K., Liu, J., Assinck, P., Bhatnagar, T., Streijger, F., Zhu, Q., Dvorak, M.F., Kwon, B.K., Tetzlaff, W., and Oxland, T.R. (2016). Differential histopathological and behavioral outcomes eight weeks after rat spinal cord injury by contusion, dislocation, and distraction mechanisms. J. Neurotrauma 33, 1667–1684.
28. Choo, A.M., Liu, J., Lam, C.K., Dvorak, M., Tetzlaff, W., and Oxland, T.R. (2007). Contusion, dislocation, and distraction: primary hemorrhage and membrane permeability in distinct mechanisms of spinal cord injury. J. Neurosurg. Spine 6, 255–266.
29. Popovich, P.G., Lemeshow, S., Gensel, J.C., and Tovar, C.A. (2012). Independent evaluation of the effects of glibenclamide on reducing progressive hemorrhagic necrosis after cervical spinal cord injury. Exp. Neurol. 233, 615–622.
30. Zhang, B., and Gensel, J.C. (2014). Is neuroinflammation in the injured spinal cord different than in the brain? Examining intrinsic differences between the brain and spinal cord. Exp. Neurol. 258, 112–120.
31. Batchelor, P.E., Tan, S., Wills, T.E., Porritt, M.J., and Howells, D.W. (2008). Comparison of inflammation in the brain and spinal cord following mechanical injury. J. Neurotrauma 25, 1217–1225.
32. Schnell, L., Fearn, S., Klassen, H., Schwab, M.E., and Perry, V.H. (1999). Acute inflammatory responses to mechanical lesions in the CNS: differences between brain and spinal cord. Eur. J. Neurosc.i 11, 3648–3658.
33. Zhang, Y.K., Liu, J.T., Peng, Z.W., Fan, H., Yao, A.H., Cheng, P., Liu, L., Ju, G., and Kuang, F. (2013). Different TLR4 expression and microglia/macrophage activation induced by hemorrhage in the rat spinal cord after compressive injury. J. Neuroinflammation 10, 112.
34. Greenhalgh, A.D., Passos Dos Santos, R., Zarruk, J.G., Salmon, C.K., Kroner, A., and David, S. (2016). Arginase-1 is expressed exclusively by infiltrating myeloid cells in CNS injury and disease. Brain Behav. Immun. 56, 61–67.
35. Getts, D.R., Terry, R.L., Getts, M.T., Deffrasnes, C., Müller, M., van Vreden, C., Ashhurst, T.M., Chami, B., McCarthy, D., Wu, H., Ma, J., Martin, A., Shae, L.D., Witting, P., Kansas, G.S., Kühn, J., Hafezi, W., Campbell, I.L., Reilly, D., Say, J., Brown, L., White, M.Y., Cordwell, S.J., Chadban, S.J., Thorp, E.B., Bao, S., Miller, S.D., and King, N.J. (2014). Therapeutic inflammatory monocyte modulation using immune-modifying microparticles. Sci. Transl. Med. 6, 219ra7.
36. Mawhinney, L.A., Thawer, S.G., Lu, W.Y., Rooijen, N.V., Weaver, L.C., Brown, A., and Dekaban, G.A. (2012). Differential detection and distribution of microglial and hematogenous macrophage populations in the injured spinal cord of lys-EGFP-ki transgenic mice. J. Neuropathol. Exp. Neurol. 71, 180–197.
37. Novakowski, K.E., Huynh, A., Han, S., Dorrington, M.G., Yin, C., Tu, Z., Pelka, P., Whyte, P., Guarné, A., Sakamoto, K., and Bowdish, D.M. (2016). A naturally occurring transcript variant of MARCO reveals the SRCR domain is critical for function. Immunol. Cell Biol. 94, 646–655.
38. Mukhopadhyay, S., Chen, Y., Sankala, M., Peiser, L., Pikkarainen, T., Kraal, G., Tryggvason, K., and Gordon, S. (2006). MARCO, an innate activation marker of macrophages, is a class A scavenger receptor for Neisseria meningitidis. Eur. J. Immunol. 36, 940–949.
39. Elomaa, O., Kangas, M., Sahlberg, C., Tuukkanen, J., Sormunen, R., Liakka, A., Thesleff, I., Kraal, G., and Tryggvason, K. (1995). Cloning of a novel bacteria-binding receptor structurally related to scavenger receptors and expressed in a subset of macrophages. Cell 80, 603–609.
40. Mukhopadhyay, S., Varin, A., Chen, Y., Liu, B., Tryggvason, K., and Gordon, S. (2011). SR-A/MARCO-mediated ligand delivery enhances intracellular TLR and NLR function, but ligand scavenging from cell surface limits TLR4 response to pathogens. Blood 117, 1319–1328.
41. Bowdish, D.M., Sakamoto, K., Kim, M.J., Kroos, M., Mukhopadhyay, S., Leifer, C.A., Tryggvason, K., Gordon, S., and Russell, D.G. (2009). MARCO, TLR2, and CD14 are required for macrophage cytokine responses to mycobacterial trehalose dimycolate and Mycobacterium tuberculosis. PLoS Pathog. 5, e1000474.
42. Dahl, M., Bauer, A.K., Arredouani, M., Soininen, R., Tryggvason, K., Kleeberger, S.R., and Kobzik, L. (2007). Protection against inhaled oxidants through scavenging of oxidized lipids by macrophage receptors MARCO and SR-AI/II. J. Clin. Invest. 117, 757–764.
43. Carlson, G.D., Minato, Y., Okada, A., Gorden, C.D., Warden, K.E., Barbeau, J.M., Biro, C.L., Bahnuik, E., Bohlman, H.H., and Lamanna, J.C. (1997). Early time-dependent decompression for spinal cord injury: vascular mechanisms of recovery. J. Neurotrauma 14, 951–962.
44. Fenn, A.M., Hall, J.C., Gensel, J.C., Popovich, P.G., and Godbout, J.P. (2014). IL-4 signaling drives a unique arginase+/IL-1β+ microglia phenotype and recruits macrophages to the inflammatory CNS: consequences of age-related deficits in IL-4Rα after traumatic spinal cord injury. J. Neurosci. 34, 8904–8917.
45. Datto, J.P., Bastidas, J.C., Miller, N.L., Shah, A.K., Arheart, K.L., Marcillo, A.E., Dietrich, W.D., and Pearse, D.D. (2015). Female rats demonstrate improved locomotor recovery and greater preservation of white and gray matter after traumatic spinal cord injury compared to males. J. Neurotrauma 32, 1146–1157.
46. Zhang, B., Bailey, W.M., Braun, K.J., and Gensel, J.C. (2015). Age decreases macrophage IL-10 expression: implications for functional recovery and tissue repair in spinal cord injury. Exp. Neurol. 273, 83–91.
47. Zhang, B., Bailey, W.M., McVicar, A.L., and Gensel, J.C. (2016). Age increases reactive oxygen species production in macrophages and potentiates oxidative damage after spinal cord injury. Neurobiol. Aging 47, 157–167.

Address correspondence to:
John C. Gensel, PhD
University of Kentucky
741 S. Limestone
B463 BBSRB
Lexington, KY 40536

E-mail: gensel.1@uky.edu